Journal of proteome research

pubs.acs.org/jpr

Article

A Multiplexed Quantitative Analysis of Germline Single Amino Acid Variants by Targeted Proteomics in Nondepleted Human Plasma

Panshak P. Dakup, Tai-Tu Lin, Soumyadeep Sarkar, Athena M. Schepmoes, Thomas L. Fillmore, Tujin Shi, Wei-Jun Qian, Jon M. Jacobs,* and A2CPS Consortium

Cite This: J. Proteome Res. 2026, 25, 2296−2307

Read Online

ACCESS | Metrics & More | Article Recommendations | Supporting Information

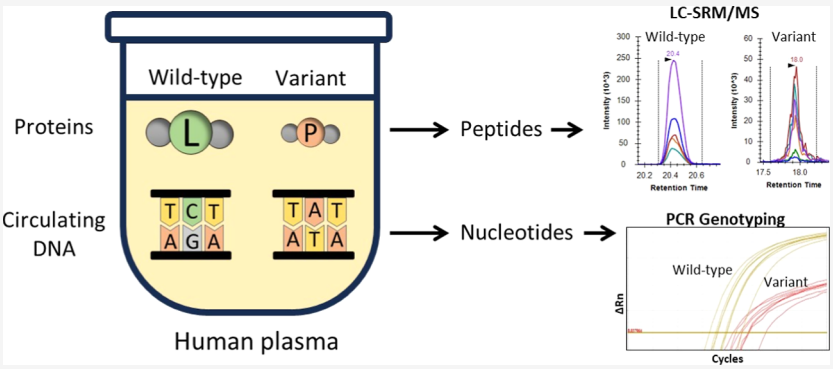

ABSTRACT: Single amino acid variants (SAAVs) in protein sequences are often a direct result of single-nucleotide polymorphisms (SNPs). Certain germline SAAVs have shown biological relevance in different disease conditions but lack precise quantification in circulation, which could hinder functional investigations and progress in biomarker development. Here, we have developed a multiplexed liquid chromatography-selected reaction monitoring (LC-SRM) assay that monitors 5 wild-type and variant peptide pairs (Complement Factor B: CFB-R32Q/R32W, Clusterin: CLU-N317H, Fetuin B: FETUB-K360R, and Kininogen: KNG1-L212P) in nondepleted human plasma. The assay was optimized for imprecision, linearity, stability, and calibration assessments with CVs of under 20%. The wild-type and variant peptide pairs were characterized in a set of healthy individual plasma samples. These target identifications were also validated by SNP genotyping with more than 99% accuracy. For all protein targets, we observed significantly lower concentrations of WT species in the presence variant peptides. In CFB, the concentration of R32Q was significantly lower than its counterpart R32W variant and WT species. Furthermore, our results distinguished phenotypes of homozygosity and heterozygosity of the SAAV presence through direct concentration level characterization. These findings provide some insights into how SAAVs affect quantitative assessments of target peptides. The assay demonstrates a platform for proteogenomic analyses with potential applications in both research and clinical settings.

KEYWORDS: *LC-MS assay, plasma, targeted proteomics, selected reaction monitoring, single amino acid variant, single nucleotide polymorphism, genotypes, Complement Factor B, Clusterin, Fetuin B, Kininogen*

1. INTRODUCTION

Protein concentration levels serve as useful indicators of physiological states and are increasingly employed as diagnostic and prognostic biomarkers. There is significant interest in expanding the utility of proteins in biomarker research. However, various factors can influence protein levels, with nonsynonymous single nucleotide polymorphisms (SNPs) being a notable contributor.[1] Millions of SNPs exist, with an approximate frequency of 1 in 1000 base pairs.[2,3] These SNPs can result in single amino acid variants (SAAVs) in protein sequences, thereby affecting their concentrations and functions.[4,5]

Our study focuses on specific germline SAAVs in four proteins—Complement Factor B (CFB), Clusterin (CLU), Fetuin B (FETUB), and Kininogen (KNG1)—which were selected as part of the Acute to Chronic Pain Signatures (A2CPS) candidate proteins due to their involvement in pain-related mechanisms.[6,7] CFB mediates inflammation and promotes nociception through the activation of complement cascades;[8] CLU has anti-apoptotic and anti-neuroinflammatory effects;[9,10] FETUB is implicated in proinflammatory signaling;[11]

Received: September 25, 2025
Revised: March 9, 2026
Accepted: March 16, 2026
Published: March 26, 2026

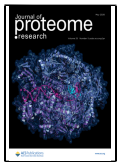

https://doi.org/10.1021/acs.jproteome.5c00928
J. Proteome Res. 2026, 25, 2296−2307

and KNG1 serves as a precursor for kinins, which directly mediate pain by sensitizing nociceptors.[12] The selected variants include R32Q and R32W in CFB, N317H in CLU, K360R in FETUB, and L212P in KNG1. Reference databases such as the Genome-Wide Association Studies (GWAS) and the National Library of Medicine's ClinVar have enabled linking genetic variants with diseases and phenotypic traits in large populations.[13−16] To mention a few, CFB R32Q and R32W have been associated with protection against age-related macular degeneration (ARMD), though R32W is also linked to conditions like atypical hemolytic-uremic syndrome, Factor B fast/slow polymorphism, and complement component 2 deficiency.[13,17−20] CLU N317H poses a risk for ischemic heart disease and has been predicted to have pathogenic potential in Alzheimer's disease.[13,21−23] FETUB K360R is a core binding factor in acute myeloid leukemia susceptibility,[13] while the outcomes of KNG1 L212P remain largely unknown (Table 1).

Historically, SNP detection has relied on genomic analyses, which, despite advancements in SNP arrays and sequencing techniques, often fall short of providing absolute quantification or insight into protein-level impacts. These methods primarily identify the presence of an SNP but do not capture how such changes affect protein abundance. This gap highlights the need for proteomic approaches to bridge genotype−phenotype relationships and investigate how SNPs influence protein concentrations in plasma—a biofluid extensively used in both research and clinical settings.

In this study, we employed targeted mass spectrometry using liquid chromatography-selected reaction monitoring (LC-SRM) to quantitatively evaluate SAAVs in nondepleted human plasma, validating our findings via genotyping (Figure 1). This method offers high specificity and versatility compared to immunoassays, which require extremely specific antibodies. A recent review of methodological advancements in SAAV detection and quantitation[24] highlighted the growing importance of proteomic approaches in characterizing these proteoforms. Previous studies within disease contexts have investigated multiple isoforms of complement factor H (CFH) in plasma from an aging cohort,[25] analyzed WT and variant sequences from CFH, complement C5, and C7 in depleted plasma from an obesity cohort,[26] and studied SAAVs from pancreatic patients serum using targeted and discovery proteomics approaches.[27] Building on these efforts, our work seeks to elucidate SNP impacts on WT concentrations in "healthy" physiological states. We characterized WT and variant peptides and mapped their genetic variety. A multiplexed LC-SRM assay was developed to quantify nine targets, consisting of four WT and five variant peptides, in nondepleted plasma from 70 healthy individuals. This study underscores the potential of targeted proteomics as a complementary approach to genomics, enabling a greater functional understanding of SNPs in physiological contexts.

2. MATERIALS AND METHODS

2.1. Peptides, Probes, and Chemicals

All peptides were synthesized and purchased from Vivitide [now Biosynth] (Gardner, MA). Internal standard peptides (crude purity) with heavy isotope labels on C-terminal lysine (K) or arginine (R) were purchased for assay development. High-purity (>99%) light standard peptides were also purchased to calibrate the heavy standards. All cysteine residues were carbamidomethylated. Urea, dithiothreitol (DTT), iodoacetamide (IAA), ammonium bicarbonate (NH_4HCO_3), trifluoroacetic acid (TFA), and formic acid (FA) were obtained from Sigma (St. Louis, MO). LC/MS-grade acetonitrile (ACN) was

Table 1. Description of target proteins, peptide sequences, and their associated genomic and biological information, retrieved from UniProt, GWAS catalog, 1000 Genomes Project, and ClinVar databases

Protein	Wild-type peptide	Variant peptide(s)	Position: codon change	SNP ID	Frequency	Associated trait
Complement Factor B (CFB)	TPWSLARPQGSCSLEGVEIK	TPWSLA**Q**PQGSCSLEGVEIK	32: R [CGG] → Q[CAG]	rs641153	12%	Protection from age-related macular degeneration
		TPWSLA**W**PQGSCSLEGVEIK	32: R [CGG] → W[TGG]	rs12614	18%	Linked to chronic kidney disease with hypertension; atypical hemolytic-uremic syndrome
Clusterin (CLU)	EILSVDCSTNNPSQAK	EILSVDCSTN**H**PSQAK	317: N[AAC] → H[CAC]	rs9331936	7%	High risk for ischemic heart disease; possibly damaging with pathogenicity prediction in Alzheimer's disease
Fetuin B (FETUB)	LVVLPFPK	LVVLPFP**R**	360: K[AAA] → R[AGA]	rs7999	6%	Susceptibility to acute myeloid leukemia; depressive symptoms
Kininogen (KNG1)	ENFLFLTPDCK	ENF**P**FLTPDCK	212: L [CTG] → P[CCG]	rs5030024	0.20%	Unknown

https://doi.org/10.1021/acs.jproteome.5c00928
J. Proteome Res. 2026, 25, 2296−2307

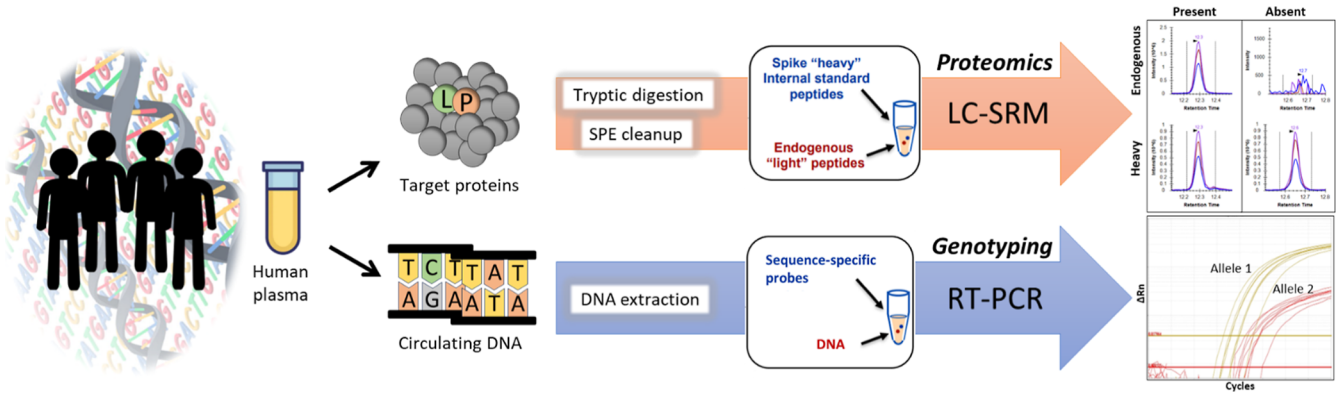

Figure 1. Rationale and study design. Complementary targeted proteomics (LC-SRM) and real-time PCR (RT-PCR) genotyping workflows to assess WT/SAAV pairs in human plasma.

obtained from Thermo Fisher Scientific (Waltham, MA), and sequencing grade trypsin was obtained from Promega (Madison, WI).

For genotyping, custom Taqman probes were synthesized and purchased from Thermo Fisher Scientific (Waltham, MA). Each custom probe was designed with primers to recognize one pair of wild-type/SNP nucleotide. Any known nontarget SNPs within the range of detection of the sequence were masked. The assay names and identifiers are as follows: CFB_R32Q: AN2XRUJ; CFB_R32W: AN33KEG; CLU_N317H: AN7D9JC; FETUB_K360R: AN9H239; KNG1_L212P: AN49EYE (Table S8). Positive control DNA sequence templates were synthesized and purchased from Integrated DNA Technologies (Coralville, IA) (Table S9). DNeasy Blood and Tissue Kits for DNA Isolation was purchased from Qiagen (Hilden, Germany).

2.2. Plasma Samples

Individual and pooled commercially available human plasma (K2EDTA anticoagulant) were purchased from BioIVT (HUMANPLK2-9981-D, Westbury, NY). These samples were from healthy donors and confirmed to be negative for pathogens or infections. A total of 70 plasma samples from healthy donors (age: 18−74 years; 49% female, 51% male; ethnicity: 34% Black, 22% Caucasian, 43% Hispanic, 1% other) were used in this study. The demographic information for each individual is provided in Table S1.

The analysis of the deidentified samples in this study was qualified as non-human subjects research by the Institutional Review Board (IRB) at Pacific Northwest National Laboratory.

2.3. Proteomic Sample Preparation

All human plasma samples used in this study were nondepleted. Briefly, 5 μL of the plasma sample was added to each well containing 45 μL of 8 M urea in 50 mM NH_4HCO_3 (ABC). Then, proteins were reduced with 10 mM DTT and incubated for 30 min at 37 °C, 1200 rpm, followed by alkylation with 40 mM IAA and incubation in the dark for 1 h at 37 °C, 1200 rpm. Samples were diluted 6-fold by adding 50 mM ABC containing $CaCl_2$ (1 mM final concentration) and digested with trypsin at an enzyme-to-substrate ratio of 1 μg of trypsin per 50 μg (1:50) of total protein. The mixture was incubated for 6 h at 37 °C, 1200 rpm after which digestion was quenched by acidifying the samples to a 0.1% TFA final concentration. Afterward, peptides were desalted by C18 SPE. C18 SPE cartridges were pre-washed with 100% MeOH and conditioned with 0.1% TFA. Peptide digests were loaded onto cartridges, washed with 95:5 H_2O:ACN and 0.1% TFA, and eluted into new 1.5 mL tubes with 80:20 ACN:H_2O, 0.1% TFA. The samples were concentrated, and BCA measurements were taken to estimate peptide concentration. The samples were then stored at −80 °C until needed.

For increased sample preparation throughput, a 96-well plate-based digestion was used. Multiple external QC samples were randomized in wells across the plate to ensure the reproducibility of the entire workflow. We followed previously established protocol for digestion and cleanup outlined in the earlier paragraph.[28] For SPE cleanup, the Strata c18-E SPE 96-well plate (Phenomenex, CA) was used. After processing, the samples were stored at −80 °C until needed.

A mix of nine heavy internal standards was prepared and spiked into every sample at the same concentrations right before the MS analysis (except as stated otherwise). The individual optimized concentrations of each target peptide are shown in Table S2.

2.4. LC-SRM

The LC-SRM analysis was performed with a nanoACQUITY UPLC system (Waters Corporation, Milford, MA) interfaced to a TSQ Altis Triple Quadrupole mass spectrometer equipped with a nano-ESI source (Thermo Scientific). An injection volume of 2 μL was used for the separation using a BEH C18 nanoACQUITY column (100 μm i.d. x 100 mm, 1.7 μm, 130 Å, Waters). Mobile phase A was 0.1% FA in water, and mobile phase B was 0.1% FA in ACN. The LC gradient started at 1% B with a flow rate of 500 nL/min, ramped up 1−6% B in 4−5 min, 6−13% B in 5−20 min, 13−22% B in 20−35 min, 22−40% B in 35−40 min, and 40−95% B in 40−42 min, maintained 95% B in 42−47 min, ramped up a 1 nL/min flow rate in 47−47.5 min with 95% B, decreased 95−50% B in 47.5−48 min, ramped up 50−95% B in 48−49 min, decreased 95−1% B in 49−50 min, and maintained 1% B at a 500 nL/min flow rate in 50−59 min. The TSQ Altis QQQ mass spectrometer was operated in positive ion mode with the ESI voltage set to 2100 V and a capillary inlet temperature of 350 °C. Tube lens voltages were obtained from automatic tuning and calibration without further optimization. Both Q1 and Q3 were set at a unit resolution of 0.7 fwhm, and Q2 gas pressure was 1.5 mTorr.

To select peptide transitions, a crude heavy peptide mixture at 250 and 500 fmol/μL was created by equally mixing stock solutions of the heavy peptides. These transitions were analyzed by LC-SRM. The SRM method used was generated with the aid of Skyline. We performed an *in silico* digestion to generate all possible y-ion transitions and predicted collision energies to build an SRM method. The heavy peptide mixtures were spiked into human peptide digests and analyzed by LC-SRM to assess any potential matrix effect or interference.

2.5. DNA Isolation and SNP Genotyping

Frozen human plasma samples were thawed, and genomic DNA was isolated from 200 μL volumes with the QIAmp DNA Blood Mini Kit (Qiagen, Hilden, Germany), according to the manufacturer's instructions and as described previously.[29] The elution volume was 30 μL. The quality and quantity of genomic DNA samples were assessed by a Nano Drop 2000 Spectrophotometer (Thermo Fisher Scientific) and stored at −80 °C until needed.

DNA samples were evaluated by real-time PCR using Taqman genotyping assays (Table S8) (Thermo Fisher Scientific). Each reaction was a total of 10 μL volume comprising 3 μL of sample genomic DNA (gDNA), 0.5 μL of Taqman probe−primer mix, 5 μL of TaqPath ProAmp Master Mix (Cat # - A30866), and 1.5 μL of water. gDNA was amplified using 50 cycles (denaturation at 95 °C for 15 s and annealing/extension at 60 °C for 60 s) on the StepOnePlus Real-Time PCR System. Reactions without DNA were used as a negative control,

https://doi.org/10.1021/acs.jproteome.5c00928
J. Proteome Res. 2026, 25, 2296−2307

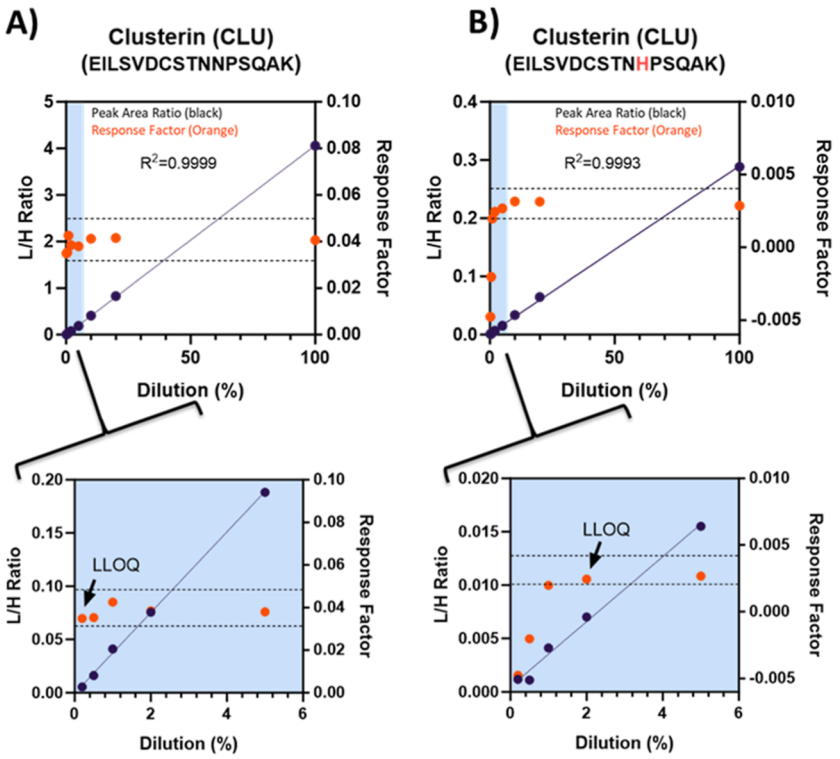

Figure 2. Linearity, response factor, and LLOQ assessment. An example of a dilution curve series for the Clusterin wild-type (WT) peptide (A) and its variant peptide (B). The expanded plots for the 0.2% to 5% human plasma dilution range are displayed below their respective full-scale curves. Black data points represent the peak area ratio (left *y*-axis), while orange data points correspond to the response factor (right *y*-axis). The LLOQ is identified as the final data point, where the response factor remains within the defined boundaries before deviating outside the acceptable range.

and reactions containing the synthesized DNA sequence for each target were used as positive controls (Table S9). The genotyping calls were reported as homozygous allele 1 or allele 2, heterozygous allele 1/2, or no amplification based on the reporter dye signal intensity normalized to ROX, passive reference dye.

2.6. Data Analysis

For SRM, generated raw data files were analyzed in Skyline. All spectra were manually inspected to ensure accurate peak detection and integration based on retention time and relative intensity ratios between light and heavy peptides. Light-to-heavy (L/H) peak area ratios were used to quantify the target peptides. These ratios were calibrated using high-purity light standards to obtain final readout endogenous peptide concentrations (μg/mL).

For PCR, fluorescent intensities of the reporter dyes were analyzed using StepOne Software v2.3. Allelic discrimination plots were generated based on the varying amplifications of each target, in addition to their alignment with the positive control reactions.

Regression analysis, grouped statistical comparisons, and image/plot generation were carried out using GraphPad Prism 10.6.0. WT versus variant concentrations comparisons were performed with two-way ANOVA and corrected for multiple comparisons with the Benjamini, Krieger, and Yekutieli method. Only groups with at least $n = 3$ were included in comparisons.

3. RESULTS

3.1. Target Peptide Selection and Identification

The proteins of interest (CFB, CLU, FETUB, and KNG1) were selected from an initial pool of 55 A2CPS candidates using a systematic selection strategy based on variant detection criteria (Supporting Information Figure S1). Tryptic peptides were selected from the Peptide Atlas database including those containing SAAVs that maintained ideal tryptic properties (e.g., length between 7 and 25 amino acids, absence of post-translational modifications (PTMs), and consistent cleavage sites between WT and SAAV forms). Table 1 summarizes the genotype frequencies, codon changes, SNP IDs, and associations with biological traits or diseases from UniProt, 1000Genomes, and Genome-Wide Association Study (GWAS) databases along with relevant literature. We also verified peptide uniqueness with neXtProt's checker tool to ensure specificity for both WT and variant forms.[30] These SNPs were found at relatively high frequencies in the population, ranging from 6% to 18%, except for KNG1 K360R, which occurs at 0.2%.

For SRM identification, we utilized *in silico* digestion via Skyline to develop an SRM method (see LC-SRM in Materials and Methods). Unique precursor ions, fragmentation patterns, and retention times allowed us to distinguish the chromatographic peaks for each target (Figure S2 and Table S3). We initially screened the top 5 to 6 transitions in approximately 0.5 μg of digested peptides from commercially pooled human plasma, and the top three were selected for the final assay (Table S3). Heavy standard peptide concentrations were optimized for the signal intensity and L/H ratio (Table S2). Detecting variant targets in pooled samples can be tricky due to frequency variations. Our targets, however, consistently exhibited L/H ratios exceeding 0.002 (CV < 20%), enabling further assay development with these samples.

3.2. SRM Assay Qualification

The assay was characterized following guidance, with minor modifications, from the Clinical Proteomics Tumor Analysis Consortium (CPTAC).[31] To achieve this, several tests were performed to assess digestion efficiency, linearity, response

https://doi.org/10.1021/acs.jproteome.5c00928
J. Proteome Res. 2026, 25, 2296−2307

Table 2. Assay qualification metrics used in SRM assay development[a]

Protein	Target peptide	Linearity	LLOQ (μg/mL)	Intra-day variability (CV) (%)	Inter-day variability (CV) (%)	Imprecision (CV_{total}) (%)	Stability (CV) (%)	Reproducibility of 96-well semiautomatic sample preparation (CV) (%)
Complement Factor B (CFB)	TPWSLARPQGSCSLEGVEIK	0.99918	0.077	11.70	14.58	18.69	5.53	19.09
	TPWSLA**Q**PQGSCSLEGVEIK	0.99758	0.314	11.28	16.22	19.76	4.06	15.90
	TPWSLA**W**PQGSCSLEGVEIK	0.99900	1.782	10.75	16.71	19.87	5.53	18.85
Clusterin (CLU)	EILSVDCSTNNPSQAK	0.99996	0.023	11.75	14.34	18.53	5.44	13.86
	EILSVDCSTN**H**PSQAK	0.99929	0.029	11.00	13.43	17.36	2.92	15.73
Fetuin B (FETUB)	LVVLPFPK	0.99986	0.002	11.14	12.50	16.74	5.10	17.34
	LVVLPFP**R**	0.99971	0.001	10.41	13.68	17.19	10.86	17.12
Kininogen (KNG1)	ENFLFLTPDCK	0.99963	0.486	10.07	15.05	18.11	4.97	14.92
	ENF**P**FLTPDCK	0.99985	0.010	11.65	15.53	19.41	7.69	14.38

[a]This table outlines the metrics used to evaluate the performance of the SRM assay. Linearity was assessed through linear regression (r^2) values, while the lower limit of quantification (LLOQ) was determined using both linear regression and response factor analysis. Repeatability was evaluated by measuring intra- and inter-day variation, which were combined to calculate total imprecision. Stability was assessed by monitoring peptide integrity over time, and reproducibility was determined through a plate-based digestion approach to validate the processing workflow. Variation across measurements was quantified using the coefficient of variation (CV).

factor, lower limit of quantification (LLOQ), stability, and reproducibility.

a. Assessment of trypsin digestion efficiency: A digestion time-course experiment was performed to evaluate whether trypsin digestion influenced quantification of WT and variant peptide pairs. Plasma samples were processed and incubated with trypsin for 30 min, 1 h, 2 h, 6 h, and overnight. At each time point, trypsin activity was quenched, and peptide digests were analyzed. All peptides exhibited relatively stable ratios across the digestion period, except for the CFB-WT peptide TPWSLARPQGSCSLEGVEIK, which decreased progressively over time (Figure S3). Furthermore, two semi-tryptic fragments generated at the R−P site showed correspondingly increasing signal intensities, indicating a digestion-dependent cleavage and semi-tryptic susceptibility of this peptide. To correct for the semi-tryptic loss of the CFB-WT peptide during digestion, a dual heavy-peptide spike-in experiment was performed on 5 replicates of pooled plasma and 5 individual samples. Heavy peptides were spiked-in before (predigestion) and after (postdigestion) our standard 6 h digestion. Comparison of pre- and post-digestion L/H ratios provided an estimated average correction factor of 8.0054 (Table S4), indicating that uncorrected concentrations were underestimated by ∼8-fold. The results indicate that while the full-length wild-type peptide TPWSLARPQGSCSLEGVEIK is not ideal for direct quantification due to the partial loss during digestion, the correction factor can be applied to estimate CFB-WT concentrations in individual samples.

b. Linearity, response factor, and LLOQ determination: An 8-point dilution series was used to evaluate the assay's linearity and LLOQ. Digested human plasma peptides were diluted into the Equine plasma peptide matrix at concentrations of 100%, 20%, 10%, 5%, 2%, 1%, 0.5%, and 0.2% (dilution ratios of 1:0, 1:5, 1:10, 1:20, 1:50, 1:100, 1:200, and 1:500, respectively). The total peptide concentration in all samples was 0.5 μg/μL, and each sample was spiked with a consistent concentration of heavy peptide mix (Supporting Information Table S2). A blank sample, consisting of heavy peptides without human peptides, was used as a negative control to account for potential interference. For the WT peptide of KNG1, the Equine matrix contains a matching sequence, which necessitated an additional dilution series in a Cavia peptide matrix for accurate linearity assessment specific to this peptide. All peptides demonstrated strong linearity, with strong correlation coefficients ($r^2 > 0.99$) between the measured ratios and peptide concentrations (Figure 2, Table 2, and Figure S4). To further evaluate data integrity, response factors were calculated to account for differences in the mass spectrometer's response across varying sample concentrations.[32] Acceptable response factors range between 0.8 and 1.2, reflecting a detector's response as reasonably close to the ideal of 1. Across a concentration range from 100% to 2% human plasma peptides, all target peptides exhibited a proportional response, with four peptides maintaining proportionality even below the 2% threshold. Using the linearity assessment and the response factor criteria, the LLOQ was determined for each individual peptide.

c. Imprecision: To evaluate variability and reproducibility of the assay, a 5 × 5 imprecision study was performed. In this study, five replicate samples were analyzed each day for five consecutive days. On each day, human peptides were divided into five replicates and spiked with a consistent concentration of heavy internal standard mix. The coefficient of variation (CV) was calculated to assess imprecision both within a single day (intra-day CV) and across all 5 days (inter-day CV). As expected, the inter-day CV values were generally higher than the intra-day CV values, reflecting the additional variability introduced by multiple assay preparations across days compared to measurements from a single preparation. Despite these differences, intra-day, inter-day, and total imprecision CV values for all peptides remained below 20% (Table 2).

d. Stability: The stability of the assay was evaluated under varying storage durations, conditions, and freeze−thaw cycles. A total of 16 sample replicates spiked with heavy

https://doi.org/10.1021/acs.jproteome.5c00928
J. Proteome Res. 2026, 25, 2296−2307

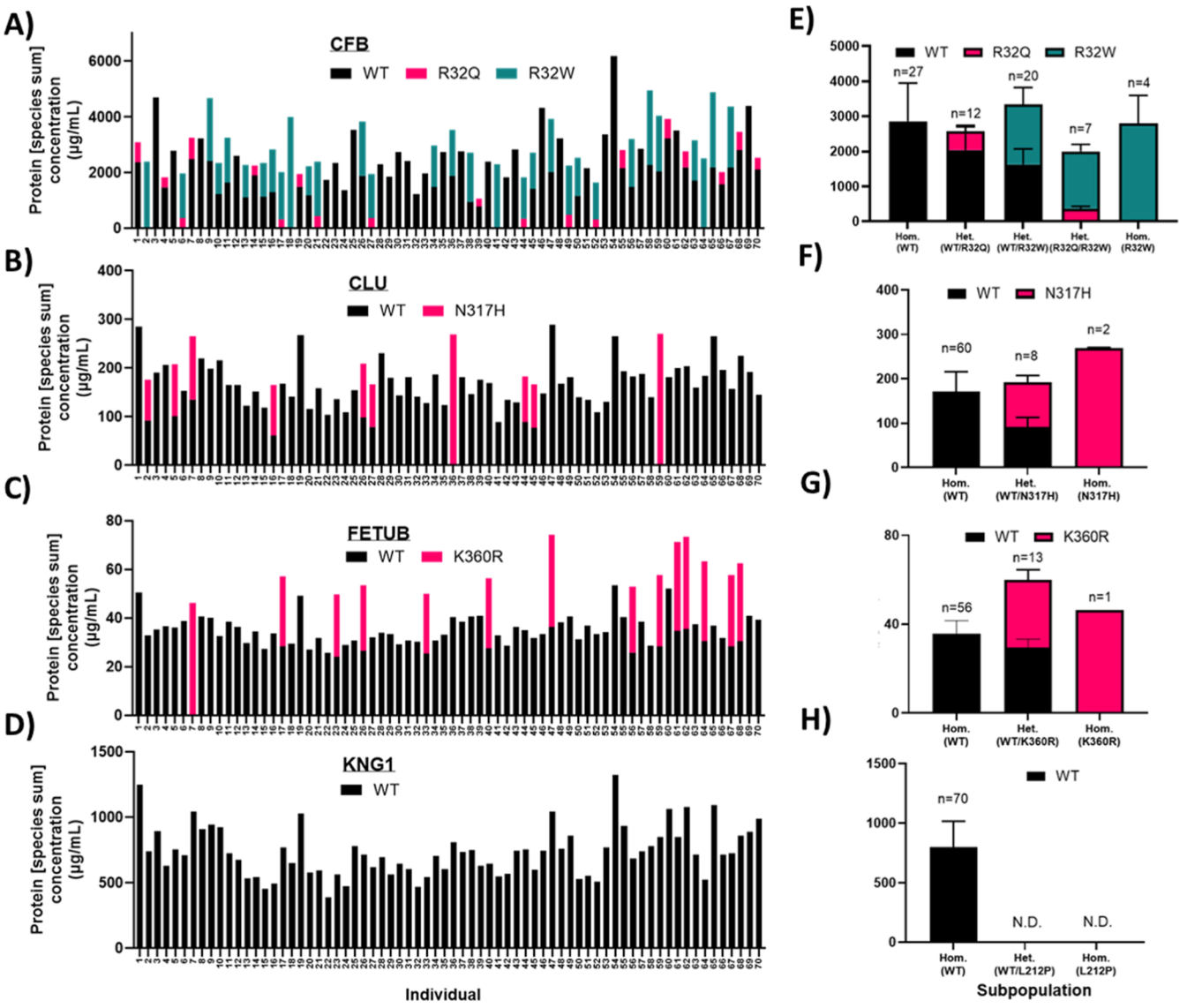

Figure 3. Variant characterization and zygosity analysis in 70 healthy human plasma samples. Characterization of WT and SAAV peptides, including their quantitative distribution patterns by concentrations (A–D). Subpopulations were further classified into homozygous and heterozygous groups (E–H). Statistical comparisons between groups are provided in Supporting Information Table S6.

peptides were prepared. For short-term stability, four vials were stored in an autosampler at 4 °C and analyzed at three time points: immediately (0 h), 24 h, and 48 h. For long-term stability, the remaining 12 vials were stored at −80 °C. At week 1, eight vials were thawed at room temperature for 1 h. Of these, four vials were analyzed after one freeze−thaw cycle, while the other four were refrozen at −80 °C. At week 2, the refrozen vials from week 1 were thawed for 1 h and analyzed after two freeze−thaw cycles. Finally, at week 4, the last four vials were thawed to room temperature and analyzed after their first freeze−thaw cycle. The stability assessment confirmed that the peptides remained stable, with coefficients of variation (CV) below 20% across all tested storage conditions, time points, and freeze−thaw cycles (Table 2).

e. Reproducibility of semi-automated plate-based sample preparation: To enable high-throughput quantification for this assay, we utilized a 96-well plate incorporating automated digestion and SPE cleanup for sample preparation. Commercially available pooled plasma samples were used for quality control and distributed across the processing plate as 18 technical replicates. These replicates were analyzed at the end of the assay to assess reproducibility. One sample was excluded from the analysis due to measurements falling outside the normal distribution range. SRM measurements from the remaining 17 pooled QC samples demonstrated good reproducibility, with coefficient of variation (CV) values below 20% across all target peptides. These results indicate reliability in the entire sample preparation and processing workflow (Table 2).

f. Quantification of protein concentration: To estimate the actual protein content in the plasma samples, an 8-point calibration curve was generated for each peptide. High-purity (>99%) light synthetic peptides at the following concentrations: 250, 50, 25, 10, 5, 2.5, 1, and 0.5 fmol/µL. These light peptides were spiked into a *Shewanella oneidensis* proteome digest matrix, along with consistent amounts of heavy peptides, and analyzed by LC-SRM. All

https://doi.org/10.1021/acs.jproteome.5c00928
J. Proteome Res. 2026, 25, 2296−2307

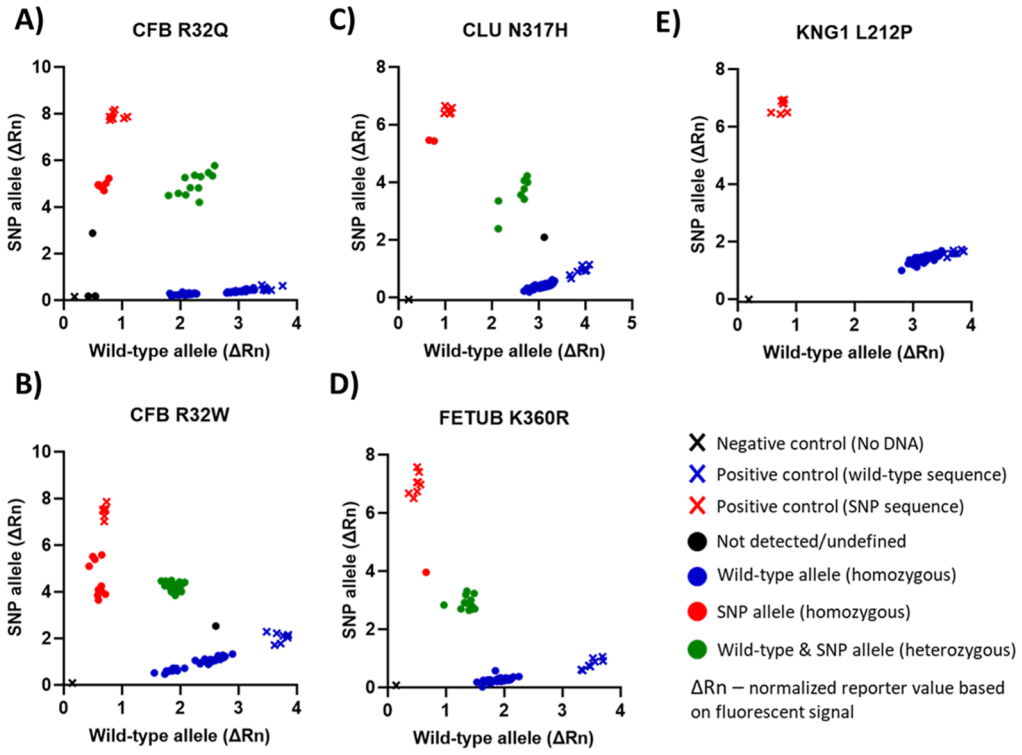

Figure 4. Validation of peptide analysis through SNP genotyping. Allelic discrimination plots for each WT/SNP pair reaction are shown. WT alleles are segregated along the *x*-axis, while SNP alleles are segregated along the *y*-axis for CFB (A-B), CLU (C), FETUB (D) and KNG1 (E). Each circle dot is DNA from a human plasma sample, and the cross represents technical controls.

peptides exhibited strong linearity, with strong correlation coefficients ($r^2 > 0.99$) between the measured ratios and pure light peptide concentrations (Figure S5). The curves were then used to adjust the L/H ratios obtained during sample analysis and estimate the protein concentration for each target peptide.

3.3. Measurements of Variants in a Healthy Population of 70 Individual Plasma Samples

To explore the concentration differences between WT and SAAV peptide pairs, we analyzed 70 plasma samples from healthy individuals. Because the SAAV peptides represent germline polymorphisms, their quantification in a healthy plasma matrix offers valuable insight into baseline expression levels and typical biological behavior. For each protein, we distinguished and quantified our WT and SAAV forms. Quantitative distribution patterns of WT and SAAV peptides are displayed in Figure 3A–D, with subpopulations further categorized into homozygous and heterozygous groups in Figure 3E-F. A demographic breakdown of the sizes of these subpopulations is provided in Table S5. Importantly, all peptide forms were accounted for across the 70 individuals, ensuring no missing data. However, the KNG1 L212P peptide was not detected in any sample, likely due to its low occurrence rate (<0.2%). Notably, sensitivity during assay optimization confirmed that the peptide could be reliably detected in pooled plasma and diluted matrices down to 2% plasma, indicating biological rarity rather than technical limitations.

In the quantitative assessment (summarized in Table S6), WT peptide concentrations were significantly lower in heterozygous individuals compared with homozygous individuals. For homozygous SAAV subpopulations, sample sizes were small across all targets, making it challenging to draw conclusive comparisons to homozygous WT individuals. However, CFB R32W was an exception, with four homozygous R32W individuals, though concentrations were not significantly different from the homozygous WT individuals.

Among heterozygous individuals, allele-specific differences were observed in the protein concentration levels. The measured ratios of WT to SAAV peptide combinations revealed distinct quantitative relationships: CFB WT/R32Q (1:0.26 ± 0.12, n = 12), CFB WT/R32W (1:1.06 ± 0.41, n = 20), CFB R32Q/R32W (1:4.39 ± 0.925, n = 7), CLU WT/N317H (1:0.83 ± 0.52, n = 8), and FETUB WT/K360R (1:0.92 ± 0.24, n = 13). When the sum of all peptide forms for each target was evaluated, trends in overall protein concentration levels varied. CLU displayed no difference, FETUB showed a moderate increase in the heterozygous individuals, while CFB saw a decrease in individuals expressing the R32Q variant. Additionally, the analysis revealed individuals heterozygous for both SAAV forms arising from the same genetic codon (e.g., CFB R32Q and R32W). This unique genotype was observed in 10% of the population, highlighting the prevalence of complex zygosity patterns.

3.4. Validation of Targeted Assay Identification of WT/SAAV Pairs

To confirm that our targeted proteomics assay accurately identified WT/SAAV peptide pairs, we employed two independent validation approaches: comparison to data from the 1000Genomes Project and a PCR-based SNP genotyping assay.[2,33]

We first compared the results of our proteomics analysis to population-level genotype data from the 1000Genomes database.[2] Using SNP IDs and nucleotide change information (Table 1), we queried the database for the occurrence of each

https://doi.org/10.1021/acs.jproteome.5c00928
J. Proteome Res. 2026, 25, 2296−2307

variant in the population. The variant frequencies identified by our proteomics assay were consistent with those reported in the 1000Genomes data set (Figure S6 and Table S7). Notably, our proteomics method provided additional resolution, enabling the detection of heterozygous-only populations as in the case of CFB R32Q and R32W heterozygous genotype.

To experimentally validate our results, we performed a real-time PCR-based SNP genotyping assay using genomic DNA extracted from the same plasma of 70 individuals. Genomic DNA was extracted, yielding an average concentration of 4 ng/μL. Custom probes specific to each WT/SAAV pair were synthesized to target DNA regions containing either the WT or SNP alleles. Negative controls (reactions without DNA) and positive controls (reactions with synthetic DNA sequence for each target) were used to ensure assay specificity. ΔRn, referring to the change in the fluorescence signal for a given reporter dye, was used to distinguish genotypes, discriminating SNP allele reporter dyes (y-axis) from WT allele reporter dyes (x-axis). Heterozygous alleles were represented by intermediate ΔRn for both dyes, creating a cluster in the middle of the plot, clearly separating them from homozygous WT and homozygous SAAV (Figure 4). Noteworthy, the results from this assay showed a 99.5% accuracy match with our targeted proteomics data, with only three mismatches identified (one each for CFB R32Q, CFB R32W, and CLU N317H).

While the PCR assay confirmed the presence of the SNP alleles, it was not possible to quantify DNA levels due to the low yield of circulating DNA from plasma. As a result, variations in the amount of input DNA for PCRs were not standardized. Despite this limitation, using the same plasma samples for both proteomic analysis and DNA extraction ensures direct alignment between protein-level quantitation and genotypic validation, minimizing discrepancies introduced by sample source variability. The strong concordance between the SNP genotyping results and proteomics readouts affirms the accuracy and specificity of our targeted proteomics assay for distinguishing WT/SAAV pairs.

In addition to the orthogonal DNA level validation, we further contextualized our protein level measurements by examining transcript level allelic effects using GTEx portal-derived Normalized Effect Sizes (NES) for each variant (Figure S7).[34] The NES values provided population-scale estimates of allele-associated changes in liver mRNA abundance, which we compared with the β coefficients derived from our plasma protein concentrations. The directionalities of variant effects as positive (increased abundance) on CLU and FETUB were aligned, but those of CFB were reversed, suggesting that the CFB may be influenced by regulatory processes downstream of transcription. This divergence is consistent with the fact that complement proteins are likely subject to hepatic secretion dynamics, alternative processing, and differential turnover, any of which could decouple plasma protein levels from transcript.[35,36]

4. DISCUSSION

In this study, we developed and applied a multiplex targeted proteomics workflow for the detection and quantification of WT and SAAV peptide pairs. By classifying individuals based on genotype and accounting for all peptide forms, we achieved a comprehensive assessment of total protein abundance. Our findings reveal that SAAVs can significantly influence protein abundance and distribution, providing new insights into genotype-dependent protein regulation and the downstream effects of SNPs on the protein level.

Our targeted assay demonstrated distinct differences in protein behavior between genotypes. In healthy individuals, heterozygous populations exhibited reduced WT peptide concentrations relative to homozygous WT populations, leading to decreased population-level protein concentrations for certain targets. By contrast, summed peptide concentrations (WT and SAAVs combined) revealed significantly reduced or elevated total protein levels in heterozygous individuals, as observed for proteins such as CFB and FETUB, respectively. Quantification of allele-specific contributions further highlighted the distinct roles of WT and SAAV species in shaping overall protein abundance. Amino acid substitutions resulting from genetic variation can alter protein structure, stability, abundance, and PTMs, ultimately impacting biological processes such as protein folding, cellular turnover, and function.[37−39]

While high-throughput genomic and transcriptomic methods (e.g., microarrays and next-generation sequencing) have enabled large-scale measurements of allele-specific expression, they lack the resolution needed to quantify the downstream proteomic effects of genetic variants.[40] Changes in peptide abundance, structure, or PTMs cannot be inferred solely from genomic data.[41] Existing proteomics approaches using isoform-specific antibodies face significant challenges with cross-reactivity, development cost, and scalability.[24] Additionally, large-scale discovery proteomics often overlooks variants, as spectral searches primarily rely on databases focused on canonical sequences.[24,42] In contrast, our MS-based targeted proteomics assay provides a quantitative, precise platform for measuring allele-specific WT and SAAV peptides in non-depleted plasma and capturing functional consequences of SNPs at the protein level. This capability streamlines assay development while enabling the robust detection of clinically relevant biomarkers. Our PCR validation at 99.5% accuracy provides orthogonal confirmation of assay specificity. Furthermore, leveraging high-pressure, high-resolution separations (e.g., PRISM-SRM) has enabled our group to quantify genetic variants at sub μg/mL levels in prostate cancer cell lines,[43] highlighting the versatility of this approach for broader clinical applications.

Despite its advantages, our current assay has certain limitations due to its peptide-centric concept. First, the current assay is limited to the selection of tryptic peptides, which restricts the method's application to targets that are predictable and measurable by trypsin digestion. Differences in trypsin digestion efficiency between SAAV and wild-type peptides may also lead to allelic imbalances, such as the significant imbalance observed in CFB R32Q and R32W which may be technical and/or biological. In our study, digestion time-course experiments revealed that the CFB WT peptide is unusually susceptible to semitryptic cleavage at the R−P bond—an exception to Keil's rule—and this systematic loss required application of an empirically derived correction factor to estimate WT concentrations.[44] Further validation experiments, such as recombinant protein digestion studies or spiked synthetic controls, could help confirm whether these observations stem from digestion biases. For candidates that do not provide suitable tryptic peptides for detection, alternative enzymes (e.g., Glu-C) could be considered. Additionally, co-modifications such as PTMs can complicate peptide-level quantification, emphasizing the need for refined workflows to untangle these overlapping signals.[45] Another challenge stems from the sequence homology within

https://doi.org/10.1021/acs.jproteome.5c00928
J. Proteome Res. 2026, 25, 2296−2307

the proteome. Variant peptide sequences that appear elsewhere may generate off-target quantification, leading to inflated concentration readings. Complementary methods, such as top-down proteomics, can address this limitation by analyzing intact proteins.[46] For example, Jager et al. successfully used top-down proteomics to distinguish alpha-1-antitrypsin variants in serum, avoiding potential interference from homologous sequences while measuring protein abundance.[47] Similarly, peptide-centric strategies like parallel reaction monitoring (PRM) with heavy, stable isotope-labeled concatemers have demonstrated the ability to precisely quantify peptide variants.[48]

Integrating RNA level information with peptide-level measurements offers additional insight into the origins of the allele specific abundance differences. In our data set, transcript-level NES values aligned with protein-level trends for CLU and FETUB, whereas CFB displayed the opposite directional pattern, indicating that transcriptional regulation alone does not fully explain its variant-associated protein behavior in circulation.[36] This divergence suggests that allele-specific abundance reflects regulatory inputs acting beyond transcription alone, including translational, post-translational, and digestion-related influences.[39] Looking forward, integrating RNA-level comparisons with SRM measurements in more controlled systems—such as single-organ or single-cell-type models—may help distinguish transcription-driven differences from tissue mixing or plasma-specific regulatory influences. These advancements highlight the potential of combining orthogonal approaches to overcome the inherent challenges of peptide-level quantification and to more fully resolve the biological significance of SAAVs.

For broader applications, PRM and data-independent acquisition (DIA) could enhance the scope and throughput of proteogenomic analyses. PRM enables high-resolution detection of fragment ions, improving specificity for co-modified or overlapping peptide sequences,[49] while DIA allows unbiased quantification in complex matrices, enabling broader profiling of noncanonical peptides, including SAAVs.[50] Both approaches complement LC-SRM workflows, particularly in studying proteins, where allelic imbalance poses a unique challenge for quantification. Furthermore, expanding the spectral search spaces to include SAAVs or noncanonical sequences could improve precision by accounting for expanding variant databases.[51] Incorporating more robust search libraries, coupled with technological adaptations, will be important for the scalability of proteogenetic research and its translation into clinical settings.

The ability to resolve WT/SAAV pairs in nondepleted plasma provides new opportunities for mechanistic and clinical studies. Its application can identify genotype-specific expression patterns across phenotypically distinct populations. Among the targets we studied, the CFB showed notable differences, with two SAAVs (R32Q and R32W) originating from the same codon but displaying dramatically different biological behaviors. Both variants have been implicated in protective roles against ARMD.[17,18] The coexistence of both SAAVs may also involve linkage disequilibrium (LD) within this genetic region.[52,53] LD describes the tendency for certain SNPs to be inherited together, which could explain the frequent detection of heterozygous individuals for both variants in our study (10% of the individuals). Understanding whether LD contributes to variant co-inheritance and its implications for phenotypes like ARMD could uncover novel insights into genotype−phenotype relationships and possible mechanisms. To explore potential mechanisms, an *ex vivo* study using mouse explants demonstrated that CFB variant proteins exhibited reduced angiogenic activity compared to the WT model.[54] Additionally, a separate study that purified plasma CFB variant proteins revealed decreased capacity to form convertase and amplify complement activation.[55] These findings suggest that the variants may influence regulatory mechanisms, potentially contributing to the pathogenesis of ARMD. However, the quantitative allelic imbalances observed in this study remain descriptive. Future studies focused on transcriptional, translational, and post-translational mechanisms are needed to uncover direct mechanistic insights into these imbalances and their impact on protein function.

5. CONCLUSION

This study demonstrates how a multiplex targeted proteomics workflow can quantitatively resolve WT and SAAV peptides directly in nondepleted human plasma. By integrating SRM-based peptide measurements with genotypic classification, we characterized allele-specific protein abundance patterns across multiple targets and revealed how common germline variants shape circulating protein levels in healthy individuals. The assay showed strong analytical performance, enabling precise quantification of variant and wild-type peptide pairs and distinguishing zygosity-dependent differences in protein abundance. These findings illustrate the value of targeted proteomics for profiling genetic variants at the protein level in circulation and provide a practical framework for expanding proteogenomic analyses in both research and clinical contexts.

■ ASSOCIATED CONTENT

Data Availability Statement

Raw MS/MS data, integrated and analyzed within Skyline files, have been deposited in Panorama under the TaMADOR-PNNL Group Site and are accessible via: Panorama Dashboard: /TAMADOR/PNNL Group/A multiplexed quantitative analysis of naturally occurring single amino acid variants by targeted proteomics in non-depleted human plasma Or https://panoramaweb.org/TAMADOR/PNNL%20Group/A%20multiplexed%20quantitative%20analysis%20of%20naturally%20occurring%20single%20amino%20acid%20variants%20by%20targeted%20proteomics%20in%20non-depleted%20human%20plasma/project-begin.view

Supporting Information

The Supporting Information is available free of charge at https://pubs.acs.org/doi/10.1021/acs.jproteome.5c00928.

Flowchart showing the candidate selection strategy (Figure S1), chromatograms of detection of peptides (Figure S2), trypsin digestion time course of plasma samples (Figure S3), peptide linearity plots (Figure S4), calibration curves for quantification (Figure S5), visual comparison of allele-specific occurrence frequencies between targeted MS detection and the 1000genomes database (Figure S6), transcript- and protein-level variant effects (Figure S7), demographics table of the 70 healthy individuals (Table S1), optimized concentrations of heavy internal standards (Table S2), assay retention times, charge states, and precursor and fragment ions (Table S3), CFB peptide correction factor calculation (Table S4), number of individuals in each genotype group by demographics (Table S5), statistical comparisons of species quantification in 70 healthy individuals (Table

https://doi.org/10.1021/acs.jproteome.5c00928
J. Proteome Res. 2026, 25, 2296−2307

S6), numerical comparison of allele-specific occurrence frequencies between targeted MS detection and the 1000genomes database (Table S7), primer−probe reporter and sequence information for SNP genotyping (Table S8), and synthesized DNA sequences used as positive controls (Table S9) (PDF)

Tables 1 to 2, and S1 to S9 are also available in excel format (XLSX)

AUTHOR INFORMATION

Corresponding Author

Jon M. Jacobs − *Environmental Molecular Sciences Laboratory, Pacific Northwest National Laboratory, Richland, Washington 99354, United States;* orcid.org/0000-0003-0557-7338; Email: Jon.Jacobs@pnnl.gov

Authors

Panshak P. Dakup − *Biological Sciences Division, Pacific Northwest National Laboratory, Richland, Washington 99354, United States;* orcid.org/0000-0003-3534-7744

Tai-Tu Lin − *Biological Sciences Division, Pacific Northwest National Laboratory, Richland, Washington 99354, United States*

Soumyadeep Sarkar − *Biological Sciences Division, Pacific Northwest National Laboratory, Richland, Washington 99354, United States;* orcid.org/0000-0002-1928-1848

Athena M. Schepmoes − *Biological Sciences Division, Pacific Northwest National Laboratory, Richland, Washington 99354, United States*

Thomas L. Fillmore − *Environmental Molecular Sciences Laboratory, Pacific Northwest National Laboratory, Richland, Washington 99354, United States*

Tujin Shi − *Biological Sciences Division, Pacific Northwest National Laboratory, Richland, Washington 99354, United States;* orcid.org/0000-0002-5592-3588

Wei-Jun Qian − *Biological Sciences Division, Pacific Northwest National Laboratory, Richland, Washington 99354, United States;* orcid.org/0000-0002-5393-2827

A2CPS Consortium − *National Institutes of Health, Bethesda, Maryland 20892, United States*

Complete contact information is available at: https://pubs.acs.org/10.1021/acs.jproteome.5c00928

Author Contributions

P.P.D., T.S., W.-J.Q., and J.M.J. conceived the study and designed experiments. A.M.S., P.P.D., T.-T.L., and T.L.F. performed sample preparation and LC-MS/MS data acquisition. P.P.D. and S.S. performed genomic-related experiments. P.P.D., T.-T.L., and S.S. statistical analysis and data visualization. T.S., W.-J.Q., and J.M.J. supervised the project. All authors contributed to the revision of the manuscript and approved the final version.

Funding

This work was supported by the Acute-to-Chronic Pain Signatures (A2CPS) Consortium: National Institute on Drug Abuse (NIDA) grant U54 DA049116 (to J.M.J. and W.-J.Q.) and the National Institute of Diabetes and Digestive and Kidney Diseases (NIDDK) grant U01 DK124020 (to W.-J.Q.). Proteomics work was performed in the Environmental Molecular Sciences Laboratory, a U.S. Department of Energy Office of Biological and Environmental Research national scientific user facility located at Pacific Northwest National Laboratory in Richland, Washington. Pacific Northwest National Laboratory is operated by Battelle for the U.S. Department of Energy under Contract No. DE-AC05-76RLO 1830.

Notes

The authors declare no competing financial interest.

ACKNOWLEDGMENTS

This study was carried out as part of the Acute to Chronic Pain Signatures (A2CPS) program, a consortium funded by the NIH Common Fund to advance research on biomarkers and mechanisms underlying the transition from acute to chronic pain. The consortium played a pivotal role in facilitating assay development through the provision of pilot samples and contributing expertise in experimental design, workflows, and quality control parameters for target detection in the context of pain-related biomarkers. The RNA-level variant data used for the analyses described in this manuscript were obtained from the GTEx Portal on 01/22/2026.

REFERENCES

(1) Robert, F.; Pelletier, J. Exploring the Impact of Single-Nucleotide Polymorphisms on Translation. *Front. Genet.* **2018**, *9*, 507.

(2) Genomes Project, C.; Abecasis, G. R.; Auton, A.; Brooks, L. D.; DePristo, M. A.; Durbin, R. M.; Handsaker, R. E.; Kang, H. M.; Marth, G. T.; McVean, G. A. An integrated map of genetic variation from 1,092 human genomes. *Nature* **2012**, *491* (7422), 56−65.

(3) McCarthy, M. I.; Abecasis, G. R.; Cardon, L. R.; Goldstein, D. B.; Little, J.; Ioannidis, J. P.; Hirschhorn, J. N. Genome-wide association studies for complex traits: consensus, uncertainty and challenges. *Nat. Rev. Genet.* **2008**, *9* (5), 356−369.

(4) Vihinen, M. Functional effects of protein variants. *Biochimie* **2021**, *180*, 104−120.

(5) Dutta, K.; Kravtsov, V.; Oleynikova, K.; Ruzov, A.; Skorb, E. V.; Shityakov, S. Analyzing the Effects of Single Nucleotide Polymorphisms on hnRNPA2/B1 Protein Stability and Function: Insights for Anticancer Therapeutic Design. *ACS Omega* **2024**, *9* (5), 5485−5495.

(6) Berardi, G.; Frey-Law, L.; Sluka, K. A.; Bayman, E. O.; Coffey, C. S.; Ecklund, D.; Vance, C. G. T.; Dailey, D. L.; Burns, J.; Buvanendran, A.; et al. Multi-Site Observational Study to Assess Biomarkers for Susceptibility or Resilience to Chronic Pain: The Acute to Chronic Pain Signatures (A2CPS) Study Protocol. *Front Med.* **2022**, *9*, 849214.

(7) Sluka, K. A.; Wager, T. D.; Sutherland, S. P.; Labosky, P. A.; Balach, T.; Bayman, E. O.; Berardi, G.; Brummett, C. M.; Burns, J.; Buvanendran, A.; et al. Predicting chronic postsurgical pain: current evidence and a novel program to develop predictive biomarker signatures. *Pain* **2023**, *164* (9), 1912−1926.

(8) Vygonskaya, M.; Wu, Y.; Price, T. J.; Chen, Z.; Smith, M. T.; Klyne, D. M.; Han, F. Y. The role and treatment potential of the complement pathway in chronic pain. *J. Pain* **2025**, *27*, 104689.

(9) Wojtas, A. M.; Carlomagno, Y.; Sens, J. P.; Kang, S. S.; Jensen, T. D.; Kurti, A.; Baker, K. E.; Berry, T. J.; Phillips, V. R.; Castanedes, M. C.; et al. Clusterin ameliorates tau pathology in vivo by inhibiting fibril formation. *Acta Neuropathol. Commun.* **2020**, *8* (1), 210.

(10) De Miguel, Z.; Khoury, N.; Betley, M. J.; Lehallier, B.; Willoughby, D.; Olsson, N.; Yang, A. C.; Hahn, O.; Lu, N.; Vest, R. T.; et al. Exercise plasma boosts memory and dampens brain inflammation via clusterin. *Nature* **2021**, *600* (7889), 494−499.

(11) Lin, K.; Wang, X.; Gu, T.; Feng, K.; Zeng, W.; Yang, L. Plasma Fetuin-B Levels are Associated with Nervous Symptoms and Conduction Velocity in Patients with Painful DPN. *Diabetes Metab Syndr Obes* **2025**, *18*, 785−793.

(12) Couture, R.; Harrisson, M.; Vianna, R. M.; Cloutier, F. Kinin receptors in pain and inflammation. *Eur. J. Pharmacol.* **2001**, *429* (1−3), 161−176.

(13) *Genome-Wide Association Studies*: National Human Genome Research Institute. https://www.ebi.ac.uk/gwas/(accessed.
(14) Manolio, T. A. Genomewide association studies and assessment of the risk of disease. *N. Engl. J. Med.* **2010**, *363* (2), 166−176.
(15) Landrum, M. J.; Lee, J. M.; Riley, G. R.; Jang, W.; Rubinstein, W. S.; Church, D. M.; Maglott, D. R. ClinVar: public archive of relationships among sequence variation and human phenotype. *Nucleic Acids Res.* **2014**, *42* (D1), D980−D985.
(16) Genome-wide association study of 14,000 cases of seven common diseases and 3,000 shared controls. *Nature* **2007**, *447* (7145), 661−678.
(17) Spencer, K. L.; Hauser, M. A.; Olson, L. M.; Schmidt, S.; Scott, W. K.; Gallins, P.; Agarwal, A.; Postel, E. A.; Pericak-Vance, M. A.; Haines, J. L. Protective effect of complement factor B and complement component 2 variants in age-related macular degeneration. *Hum. Mol. Genet.* **2007**, *16* (16), 1986−1992.
(18) Hughes, A. E.; Mullan, G. M.; Bradley, D. T. Complement factor B polymorphism 32W protects against age-related macular degeneration. *Mol. Vis* **2011**, *17*, 983−988.
(19) Mantel, I.; Ambresin, A.; Moetteli, L.; Droz, I.; Roduit, R.; Munier, F. L.; Schorderet, D. F. Complement factor B polymorphism and the phenotype of early age-related macular degeneration. *Ophthalmic Genet.* **2014**, *35* (1), 12−17.
(20) Gold, B.; Merriam, J. E.; Zernant, J.; Hancox, L. S.; Taiber, A. J.; Gehrs, K.; Cramer, K.; Neel, J.; Bergeron, J.; Barile, G. R.; et al. Variation in factor B (BF) and complement component 2 (C2) genes is associated with age-related macular degeneration. *Nat. Genet.* **2006**, *38* (4), 458−462.
(21) Bettens, K.; Brouwers, N.; Engelborghs, S.; Lambert, J. C.; Rogaeva, E.; Vandenberghe, R.; Le Bastard, N.; Pasquier, F.; Vermeulen, S.; Van Dongen, J.; et al. Both common variations and rare non-synonymous substitutions and small insertion/deletions in CLU are associated with increased Alzheimer risk. *Mol. Neurodegener.* **2012**, *7*, 3.
(22) Guerreiro, R. J.; Beck, J.; Gibbs, J. R.; Santana, I.; Rossor, M. N.; Schott, J. M.; Nalls, M. A.; Ribeiro, H.; Santiago, B.; Fox, N. C.; et al. Genetic variability in CLU and its association with Alzheimer's disease. *PLoS One* **2010**, *5* (3), No. e9510.
(23) Frikke-Schmidt, R.; Tybjaerg-Hansen, A.; Dyson, G.; Haase, C. L.; Benn, M.; Nordestgaard, B. G.; Sing, C. F. Subgroups at high risk for ischaemic heart disease:identification and validation in 67 000 individuals from the general population. *Int. J. Epidemiol* **2015**, *44* (1), 117−128.
(24) Lin, T. T.; Zhang, T.; Kitata, R. B.; Liu, T.; Smith, R. D.; Qian, W. J.; Shi, T. Mass spectrometry-based targeted proteomics for analysis of protein mutations. *Mass Spectrom. Rev.* **2023**, *42* (2), 796−821.
(25) Zhang, P.; Zhu, M.; Geng-Spyropoulos, M.; Shardell, M.; Gonzalez-Freire, M.; Gudnason, V.; Eiriksdottir, G.; Schaumberg, D.; Van Eyk, J. E.; Ferrucci, L.; et al. A novel, multiplexed targeted mass spectrometry assay for quantification of complement factor H (CFH) variants and CFH-related proteins 1−5 in human plasma. *Proteomics* **2017**, *17* (6), 1600237.
(26) Su, Z. D.; Sun, L.; Yu, D. X.; Li, R. X.; Li, H. X.; Yu, Z. J.; Sheng, Q. H.; Lin, X.; Zeng, R.; Wu, J. R. Quantitative detection of single amino acid polymorphisms by targeted proteomics. *J. Mol. Cell Biol.* **2011**, *3* (5), 309−315.
(27) Nie, S.; Yin, H.; Tan, Z.; Anderson, M. A.; Ruffin, M. T.; Simeone, D. M.; Lubman, D. M. Quantitative analysis of single amino acid variant peptides associated with pancreatic cancer in serum by an isobaric labeling quantitative method. *J. Proteome Res.* **2014**, *13* (12), 6058−6066.
(28) Lee, J. Y.; Shi, T.; Petyuk, V. A.; Schepmoes, A. A.; Fillmore, T. L.; Wang, Y. T.; Cardoni, W.; Coppit, G.; Srivastava, S.; Goodman, J. F.; et al. Detection of Head and Neck Cancer Based on Longitudinal Changes in Serum Protein Abundance. *Cancer Epidemiol., Biomarkers Prev.* **2020**, *29* (8), 1665−1672.
(29) Cheli, S.; Napoli, A.; Clementi, E.; Montrasio, C. DNA extraction from fresh and frozen plasma: an alternative for real-time PCR genotyping in pharmacogenetics. *Mol. Biol. Rep.* **2020**, *47* (8), 6451−6455.
(30) Schaeffer, M.; Gateau, A.; Teixeira, D.; Michel, P. A.; Zahn-Zabal, M.; Lane, L. The neXtProt peptide uniqueness checker: a tool for the proteomics community. *Bioinformatics* **2017**, *33* (21), 3471−3472.
(31) Song, E.; Gao, Y.; Wu, C.; Shi, T.; Nie, S.; Fillmore, T. L.; Schepmoes, A. A.; Gritsenko, M. A.; Qian, W. J.; Smith, R. D.; et al. Targeted proteomic assays for quantitation of proteins identified by proteogenomic analysis of ovarian cancer. *Sci. Data* **2017**, *4*, 170091.
(32) Reviewed, P. A practical guide to analytical method validation, including measurement uncertainty and accuracy profiles. *TrAC, Trends Anal. Chem.* **2007**, *26* (3), 227−238.
(33) Shen, G. Q.; Abdullah, K. G.; Wang, Q. K. The TaqMan method for SNP genotyping. *Methods Mol. Biol.* **2009**, *578*, 293−306.
(34) Consortium, G. T. The Genotype-Tissue Expression (GTEx) project. *Biopreserv. Biobanking* **2015**, *13* (5), 307−308.
(35) Minta, J. O.; Fung, M.; Paramaswara, B. Transcriptional and post-transcriptional regulation of complement factor I (CFI) gene expression in Hep G2 cells by interleukin-6. *Biochim. Biophys. Acta Gen. Subj.* **1998**, *1442* (2−3), 286−295.
(36) Franks, A.; Airoldi, E.; Slavov, N. Post-transcriptional regulation across human tissues. *PLoS Comput. Biol.* **2017**, *13* (5), No. e1005535.
(37) Wu, L.; Snyder, M. Impact of allele-specific peptides in proteome quantification. *Proteomics Clin Appl.* **2015**, *9* (3−4), 432−436.
(38) Wang, Z.; Moult, J. SNPs, protein structure, and disease. *Hum. Mutat.* **2001**, *17* (4), 263−270.
(39) Liu, Y.; Beyer, A.; Aebersold, R. On the Dependency of Cellular Protein Levels on mRNA Abundance. *Cell* **2016**, *165* (3), 535−550.
(40) Cleary, S.; Seoighe, C. Perspectives on Allele-Specific Expression. *Annu. Rev. Biomed Data Sci.* **2021**, *4*, 101−122.
(41) Timp, W.; Timp, G. Beyond mass spectrometry, the next step in proteomics. *Sci. Adv.* **2020**, *6* (2), No. eaax8978.
(42) Sheynkman, G. M.; Shortreed, M. R.; Frey, B. L.; Scalf, M.; Smith, L. M. Large-scale mass spectrometric detection of variant peptides resulting from nonsynonymous nucleotide differences. *J. Proteome Res.* **2014**, *13* (1), 228−240.
(43) Wang, H.; Barbieri, C. E.; He, J.; Gao, Y.; Shi, T.; Wu, C.; Schepmoes, A. A.; Fillmore, T. L.; Chae, S. S.; Huang, D.; et al. Quantification of mutant SPOP proteins in prostate cancer using mass spectrometry-based targeted proteomics. *J. Transl. Med.* **2017**, *15* (1), 175.
(44) Rodriguez, J.; Gupta, N.; Smith, R. D.; Pevzner, P. A. Does trypsin cut before proline? *J. Proteome Res.* **2008**, *7* (1), 300−305.
(45) El Kennani, S.; Crespo, M.; Govin, J.; Pflieger, D. Proteomic Analysis of Histone Variants and Their PTMs: Strategies and Pitfalls. *Proteomes* **2018**, *6* (3), 29.
(46) Roberts, D. S.; Loo, J. A.; Tsybin, Y. O.; Liu, X.; Wu, S.; Chamot-Rooke, J.; Agar, J. N.; Pasa-Tolic, L.; Smith, L. M.; Ge, Y. Top-down proteomics. *Nat. Rev. Methods Primers* **2024**, *4* (1), 38.
(47) Jager, S.; Cramer, D. A. T.; Heck, A. J. R. Normal Alpha-1-Antitrypsin Variants Display in Serum Allele-Specific Protein Levels. *J. Proteome Res.* **2023**, *22* (4), 1331−1338.
(48) Shi, J.; Wang, X.; Zhu, H.; Jiang, H.; Wang, D.; Nesvizhskii, A.; Zhu, H. J. Determining Allele-Specific Protein Expression (ASPE) Using a Novel Quantitative Concatamer Based Proteomics Method. *J. Proteome Res.* **2018**, *17* (10), 3606−3612.
(49) Peterson, A. C.; Russell, J. D.; Bailey, D. J.; Westphall, M. S.; Coon, J. J. Parallel reaction monitoring for high resolution and high mass accuracy quantitative, targeted proteomics. *Mol. Cell. Proteomics* **2012**, *11* (11), 1475−1488.
(50) Searle, B. C.; Pino, L. K.; Egertson, J. D.; Ting, Y. S.; Lawrence, R. T.; MacLean, B. X.; Villen, J.; MacCoss, M. J. Chromatogram libraries improve peptide detection and quantification by data independent acquisition mass spectrometry. *Nat. Commun.* **2018**, *9* (1), 5128.
(51) Chick, J. M.; Munger, S. C.; Simecek, P.; Huttlin, E. L.; Choi, K.; Gatti, D. M.; Raghupathy, N.; Svenson, K. L.; Churchill, G. A.; Gygi, S. P. Defining the consequences of genetic variation on a proteome-wide scale. *Nature* **2016**, *534* (7608), 500−505.

https://doi.org/10.1021/acs.jproteome.5c00928
J. Proteome Res. 2026, 25, 2296−2307

(52) Slatkin, M. Linkage disequilibrium–understanding the evolutionary past and mapping the medical future. *Nat. Rev. Genet.* **2008**, *9* (6), 477−485.
(53) Stephens, J. C.; Schneider, J. A.; Tanguay, D. A.; Choi, J.; Acharya, T.; Stanley, S. E.; Jiang, R.; Messer, C. J.; Chew, A.; Han, J. H.; et al. Haplotype variation and linkage disequilibrium in 313 human genes. *Science* **2001**, *293* (5529), 489−493.
(54) Pilotti, C.; Greenwood, J.; Moss, S. E. Functional Evaluation of AMD-Associated Risk Variants of Complement Factor B. *Invest Ophthalmol Vis Sci.* **2020**, *61* (5), 19.
(55) Montes, T.; Tortajada, A.; Morgan, B. P.; Rodriguez de Cordoba, S.; Harris, C. L. Functional basis of protection against age-related macular degeneration conferred by a common polymorphism in complement factor B. *Proc. Natl. Acad. Sci. U. S. A.* **2009**, *106* (11), 4366−4371.

https://doi.org/10.1021/acs.jproteome.5c00928
J. Proteome Res. 2026, 25, 2296−2307